

# Monensin Disruption of Neutrophil Granule Genesis

RICHARD T. PARMLEY, MD,  
JOSEPH M. KINKADE, Jr., PhD,\*  
DIANNE T. AKIN, PhD,\* CHARLES S. GILBERT,  
and GEORGIANNA S. GUZMAN\*

From the Department of Pediatrics, University of Texas Health Science Center at San Antonio, San Antonio, Texas, and the Department of Biochemistry, Emory University School of Medicine, Atlanta, Georgia\*

The  $\text{Na}^+/\text{H}^+$  ionophore monensin (M) has been used widely to study intracellular pH gradients and acidic subcellular compartments. In the present study, cultured myeloid leukemia HL60 cells, directly sampled bone marrow cells, and peripheral blood neutrophils were exposed to 1–5  $\mu\text{M}$  monensin for 0.5–20 hours. The effects were evaluated using ultrastructural, cytochemical, and biochemical methods. In HL60 cells and marrow promyelocytes treated with monensin, progressive vacuolation of the trans then the cis Golgi was observed. These vacuoles lacked diaminobenzidine (DAB) reactive peroxidase, high iron diamine (HID) reactive sulfated glycoconjugates, and periodate-thiocarbohydrazide-silver proteinate (PA-TCH-SP) reactive vicinal glycol containing complex carbohydrates, but some cis Golgi elements retained osmium zinc iodide reactive reducing groups. The number of normal intensely stained HID reactive granules decreased and an incomplete granule that was DAB-positive/HID-negative, PA-TCH-SP-negative with flocculent matrix

density increased in frequency as a function of time and concentration of monensin. Treatment of HL60 cells with monensin markedly reduced  $^{35}\text{SO}_4$  incorporation but myeloperoxidase labeling and activity per cell remained constant, although it shifted to lower density granule fractions consistent with the persistent DAB staining of endoplasmic reticulum and synthesis of a DAB-positive, HID-negative granule in intact HL60 cells. The Golgi complex of monensin-treated myelocytes and segmented neutrophils was also vacuolated. A subpopulation of preformed primary granules in promyelocytes, myelocytes, and segmented neutrophils appeared to increase in size and peripheral or central electron lucency. These selective effects of monensin indicate that granule components may be packaged into DAB-positive organelles that are deficient in trans Golgi-derived elements (HID- and PA-TCH-SP-negative) and that some preformed primary granules contain a monensin sensitive  $\text{Na}^+/\text{H}^+$  gradient. (Am J Pathol 1988, 133:537–548)

MONENSIN, A MONOVALENT carboxylic ionophore of fungal origin, disrupts  $\text{Na}^+/\text{H}^+$  gradients and has been used widely to assess the function of cellular acidic compartments.<sup>1</sup> Proton pumps have been identified as integral components of coated vesicles,<sup>2</sup> the Golgi apparatus,<sup>3</sup> lysosomes,<sup>4</sup> and secretory granules.<sup>5</sup> As a result of disruption of the proton pump, monensin has a profound inhibitory effect on the processing of macromolecules in the Golgi compartment and inhibits or dramatically alters the packaging of macromolecules into secretory<sup>6,7</sup> and lysosomal granules.<sup>8</sup> Monensin also disrupts trafficking of membrane receptors through the Golgi apparatus<sup>9</sup> and inhibits processing of viral glycoproteins<sup>10</sup> in infected cells. Previous ultrastructural studies of monensin-treated islet cells have demonstrated dramatic vacuolation of the

Golgi apparatus with the trans Golgi appearing more sensitive than the cis Golgi.<sup>6,7</sup>

Myeloid precursors and neutrophils appear to have several acidic compartments sensitive to monensin treatment. Recent studies by Akin and Kinkade<sup>11</sup> have shown that monensin inhibits processing of myeloperoxidase (MPO), resulting in accumulation of intracellular MPO precursors. The respiratory burst of neutrophils requires a  $\text{Na}^+/\text{H}^+$  antiporter, however,

Supported by USPHS Grant CA-22294 from NIH/NCI.  
Accepted for publication August 4, 1988.

Address reprint requests to Richard T. Parmley, MD, University of Texas Health Science Center at San Antonio, Department of Pediatrics, 7703 Floyd Curl Drive, San Antonio, TX 78284-7810.

Table 1—Ultrastructural Cytochemistry of Monensin Treated HL60 Cells and Marrow Promyelocytes

	Frequency		Staining characteristics of organelle matrix material*				
	Control	Monensin-treated 3–7 hours	UALC†	DAB (M/HL60)†	HID	PA-TCH-SP	OZI (M/HL60)
Endoplasmic reticulum	Abundant	Abundant	±	0–2 <sup>+</sup> /2 <sup>+</sup> ‡	0	0	0–2†/±‡
Golgi lamellae							
Cis lamellae	2–3/cell profile	<1/cell profile	0	0–2+/±	0	0	3+
Cis vacuoles	None	2–10/cell profile	0	0	0	0	0–2+
Trans lamellae	2–3/cell profile	None	±	0–2+/0	±	1–3+	0
Trans vacuoles	0–2/cell profile	5–10/cell profile	0	0	0	0	0
Coated vesicles	2–30/cell profile	Unchanged	Sparse	±	0	1–3+	0–2+
Condensing vacuoles	2–5/cell profile	Rare	Sparse	2+	2+	2+	0
Incomplete granule	Rare	5–20/cell profile	Heterogeneous (±vesicles)	2+	0	0	1+
Immature granule	2–30/cell profile	Rare	Heterogeneous	3+	3+	3+	0
Mature granule (marrow only)	0–40/cell profile	0–20/cell profile	Homogeneous	3+	±	±	0
Expanded granule	Rare	1–20/cell profile	Central and/or rim density	2+	0–3+	±	±§

\* Staining graded 0 (no staining), ± (weak staining in some organelles), 1+ (weak staining) to 3+ (strong staining).

† UALC, uranyl acetate and lead citrate; M, marrow.

‡ DAB and OZI staining of endoplasmic reticulum progressively decreased in marrow cells incubated in control solutions for greater than 3 hours.

§ OZI staining was present in vesiclelike foci in the periphery of some expanded granules.

the Na<sup>+</sup> influx created by monensin alone fails to activate superoxide production.<sup>12</sup> The monensin-induced Na<sup>+</sup> influx and H<sup>+</sup> efflux is comparable with that produced with N-formyl-methionyl-leucyl-phenylalanine (FMLP).<sup>13,14</sup> Although monensin inhibits receptor-mediated FMLP uptake and chemotaxis, it has little effect on FMLP stimulated superoxide production, suggesting that Golgi mediated receptor processing is important for the former functions but not the latter.<sup>9</sup> The purpose of the present study was to identify specific morphologic compartments altered by monensin and assess the effects of monensin on neutrophil granules in normal bone marrow, peripheral blood, and cultured HL60 cells. A preliminary report of parts of this study has been published previously.<sup>15</sup>

## Materials and Methods

### Specimen Preparation and Exposure to Monensin

HL60 cells were grown in RPMI 1640 medium supplemented with 10% defined bovine calf serum (BCS, HyClone Laboratories, Logan, UT) in 7.5% CO<sub>2</sub> in air at 37 C. Cells were subcultured twice weekly at an initial density of 2.5 × 10<sup>5</sup> cells/ml and were harvested for experiments after 3–4 days in culture and counted in a hemocytometer. All experiments were performed with cells between passage 20 and 47. Bone marrow cells were obtained by needle aspiration in heparin after informed consent from a normal donor (N = 1) and during routine staging of patients with solid tumors not involving bone marrow or leukemia in remission and off chemotherapy (N = 2). Peripheral

blood was obtained from normal volunteers by phlebotomy in heparinized syringes (N = 3). Bone marrow aspirates were added directly to RPMI 1640 medium (Sigma Chemical Co., St. Louis, MO) containing 5 units/ml heparin (Sigma Chemical Co.). Marrow suspensions were layered over 2 ml Ficoll Hypaque (Sigma Chemical Co., specific gravity 1.077) and centrifuged for 30 minutes at 400g. The light density cells were recovered and washed once in RPMI medium containing 10% BCS. In some cases, marrow buffy coat cells were recovered from the marrow suspension after centrifugation at 580g for 10 minutes. Neutrophils and nucleated cells were suspended at 10<sup>6</sup>/ml in RPMI 1640 medium containing 10% BCS and were incubated for the indicated period of time at 37 C in an atmosphere of 7.5% CO<sub>2</sub> with and without 1–5 μM monensin (Sigma Chemical Co.). The monensin was prepared as a stock solution (1 mM) in 95% ethanol and 1–5 μl were added to each ml of the cell incubation mixture. Control samples received an equivalent amount of 95% ethanol. Marrow and blood cell samples were incubated for 30 minutes, 1, 3, and 7 hours. HL60 cells were incubated for these time intervals, as well as a 20-hour time interval. The incubation was stopped by placing the cells on ice and cells were recovered by centrifugation at 250g for 7 minutes at 4 C and fixed for electron microscopy as described below.

### Electron Microscopy

HL-60 cells, bone marrow, and blood cells were resuspended in 10–15 volumes of ice cold fixing solu-

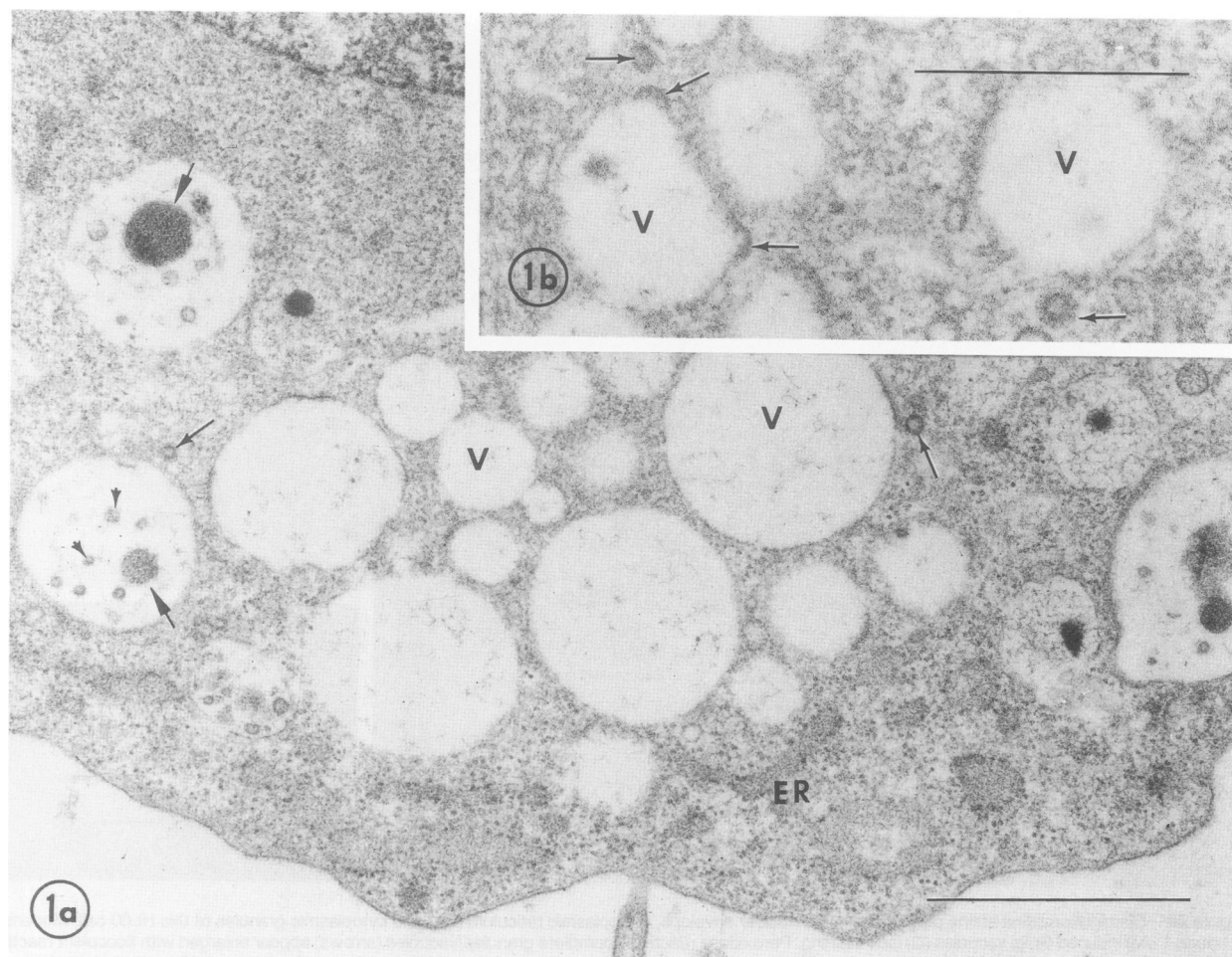


**Figure 1**—After 3 hours exposure to monensin ( $1 \mu\text{M}$ ) this HL60 cell (a) contains prominent cytoplasmic vacuoles (V) in the Golgi region. These vacuoles are flanked by vacuolated structures that appear to contain membrane limited vesicles (arrow heads) and apparent granule matrix material (large arrows). Alternatively, these apparent intragranular vesicle profiles could represent indentations into granules created by granule vesicle fusion. Endoplasmic reticulum (ER) appears unaltered compared to untreated cells. Several coated vesicles are evident (small arrows, enlarged in b) and some appear to have fused with cytoplasmic vacuolated structures (V, small arrows). Nucleus (N). Thin section stained with uranyl acetate and lead citrate. Bar =  $1 \mu$ ; inset bar =  $0.5 \mu$ .

tion (3% glutaraldehyde in 0.1 M cacodylate buffer, pH 7.35) by gentle aspiration through a 28-gauge needle three times. The cells were kept in the fixative at 4 C for 1 hour and then were washed three times in 0.1 M cacodylate buffer containing 7 g/dl sucrose, pH 7.35. Some samples were fixed in 3% agar using the same conditions except that the tissues were minced during fixation using a razor blade. The samples were then rinsed three times in 0.1 M cacodylate, 7 g/dl sucrose, pH 7.35. Samples for peroxidase staining were incubated 30 minutes in 10 ml of 0.05 M Tris HCl buffer, pH 7.6, containing 5 mg of 3,3' diaminobenzidine·4 HCl (Sigma Chemical Co.) and 0.01%  $\text{H}_2\text{O}_2$  as described previously.<sup>16</sup> Specimens to be subsequently stained for vicinal glycols were incubated in porcine alpha-amylase (Sigma Chemical Co.) as described previously.<sup>17</sup> Reducing substances were

stained with the osmium zinc iodide (OZI) method according to Clark and Ackerman.<sup>18</sup> Sulfated glycoconjugates were stained with Spicer's high iron diamine (HID) method before embedment as described previously.<sup>19,20</sup> Morphology and peroxidase-stained specimens were postfixed 1 hour in 1%  $\text{OsO}_4$  in 0.1 M cacodylate, pH 7.35. All samples were routinely dehydrated in graded alcohols and propylene oxide and embedded in Spurr low viscosity medium (Polysciences, Warrington, PA).

Thin sections 50–70 nm thick were obtained with a diamond knife. Specimens stained for complex carbohydrates (vicinal glycols and sulfated glycoconjugates) were collected on stainless steel grids. Vicinal glycol staining was accomplished by sequential exposure of grids to periodate, thiocarbohydrazide (Schiff reagent) and silver proteinate (PA-TCH-SP) as described pre-

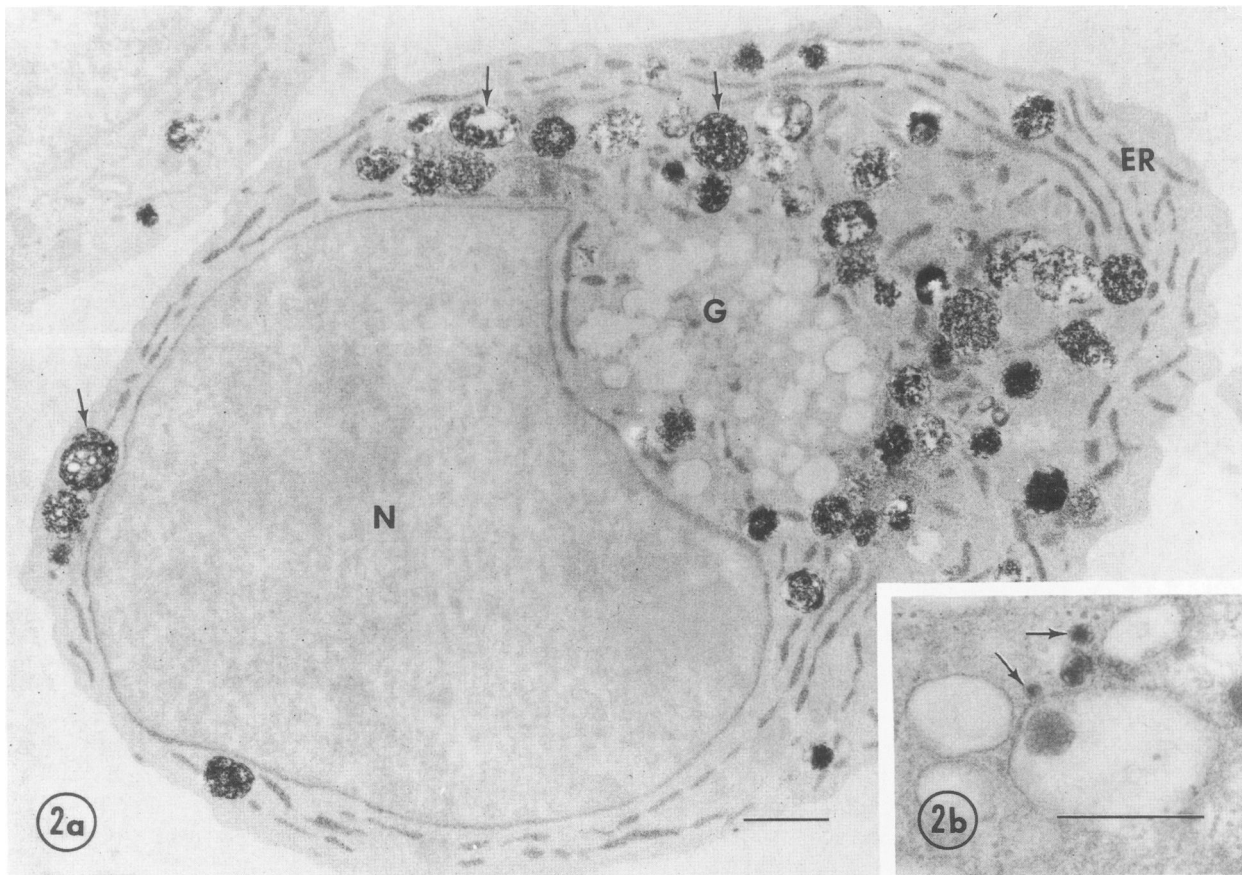


**Figure 2a**—Diaminobenzidine stains peroxidase in the nuclear envelope, endoplasmic reticulum (ER) and cytoplasmic granules of this HL60 cell. Monensin (7 hours, 1  $\mu$ M) induced Golgi vacuoles (G) lack staining. Peroxidase reactive incomplete granules/vacuoles (arrows) appear enlarged with flocculent reactive densities not seen in untreated HL60 cells. **b**—Enlargement of a portion of a similar cell demonstrating activity in some cytoplasmic vesicles (arrows) bordering monensin induced vacuolated structures and a presumed incomplete granule. N, nucleus. a, thin section not counterstained. b, counterstained with lead citrate. Bar = 1  $\mu$ ; inset bar = 0.5  $\mu$ .

viously.<sup>17,21</sup> HID staining of sulfated glycoconjugates was enhanced by exposure to TCH-SP as described previously.<sup>20,22</sup> All specimens were examined in a Zeiss EM 109 electron microscope at an accelerating voltage of 50 kV.

### Biochemical Analytic Methods

HL60 cells were grown (16–20 hours) in the presence or absence (control) of 1  $\mu$ M monensin as described above. General protein and myeloperoxidase synthesis were measured by pulse-labeling HL60 cells with [<sup>35</sup>S]methionine and determining incorporation into total trichloroacetic acid-precipitable protein as described previously.<sup>23</sup> Myeloperoxidase activity was determined using guaiacol as the electron donor by measuring the absorbance change at 470 nm as described earlier.<sup>24</sup> The activities of  $\beta$ -glucuronidase and acid phosphatase were determined as reported previously,<sup>25,26</sup> using phenolphthalein glucuronic

acid and phenolphthalein- $\beta$ -glycerophosphate (Sigma Chemical Co.) respectively, as substrates. Labeling of Golgi and granule compartments with [<sup>35</sup>S]O<sub>4</sub> (sodium salt) was carried out as described previously.<sup>26</sup> All values were initially calculated on a per cell basis. The distribution of myeloperoxidase and  $\beta$ -glucuronidase in different subcellular fractions was accomplished after Percoll density gradient centrifugation of the post-nuclear supernatant from both pulse-labeled and unlabeled cells as described previously.<sup>26</sup>

## Results

### HL60 Cells

The ultrastructural morphology and cytochemistry of HL60 cells, not exposed to monensin, resembled that described previously,<sup>27</sup> and is summarized in Table 1.

Increasing cytoplasmic abnormalities were noted with time after exposure to monensin (Table 1). These

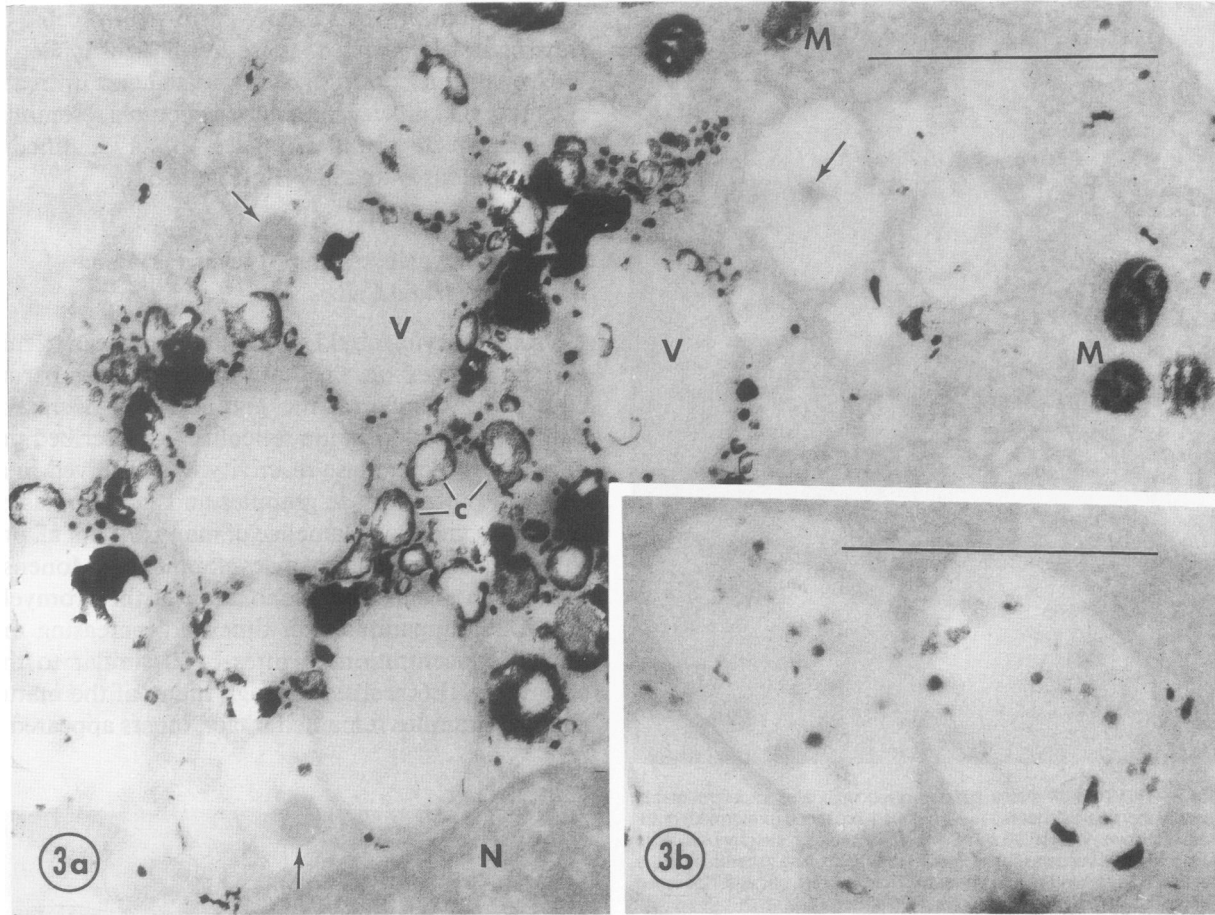


**Figure 3**—OZI strongly stains reducing groups in cytoplasmic vesicles and minimally dilated cis Golgi elements (c) of this monensin (3 hours, 5  $\mu$ M) treated HL60 cell (a). Large vacuoles (V) presumably correspond to trans Golgi elements and incomplete granules. Incomplete granules contain variable amounts of OZI reactive foci (enlarged in b) some of which correspond to vesicle-like structures seen in morphologic preparations (cf Figure 1). Residual granule matrix material (arrows) of monensin expanded granules lack staining. Mitochondria (M) stain intensely. N, nucleus. Thin section not counterstained. Bars = 1  $\mu$ .

changes were largely limited to vacuolation of the trans Golgi within 30–60 minutes of exposure to monensin. After 3–7 hours this vacuolation increased to involve the cis and trans Golgi (Figures 1, 2). The Golgi vacuolation remained prominent after 20 hours of exposure to monensin. Cells appeared intact in samples treated up to 20 hours with 1  $\mu$ M monensin, however, cell integrity was compromised by exposure to 5  $\mu$ M monensin in the 20-hour specimen. The monensin induced Golgi vacuoles demonstrated variable OZI staining (Figure 3), which was strongest in cis Golgi elements but lacked DAB staining (Figure 2), PA-TCH-SP, and HID-TCH-SP (Figure 4) staining.

The number of condensed cytoplasmic granules stained with DAB, PA-TCH-SP, and HID-TCH-SP progressively decreased with time (and increased monensin concentration) after exposure to monensin. An increase in cytoplasmic granules, termed expanded granules, was observed in these same cells. The expanded granules contained an exaggerated

electron-lucent rim and an eccentric or central dense residual matrix that appeared DAB positive and variably HID-TCH-SP reactive (Figures 2, 4). There was also a progressive increase in granules/vacuoles that contained flocculent matrix density and/or a few to abundant vesicles and were termed incomplete granules (Figure 1). These incomplete granules were DAB positive but lacked HID-TCH-SP and PA-TCH-SP-stained glycoconjugates (Figures 2, 4). These incomplete granules often contained OZI reactive vesicles (Figure 3).

Endoplasmic reticulum (Figures 2, 5a) and coated vesicles (Figure 1) were observed and appeared similar in both monensin and control samples. Presumably some of these vesicles were derived from endoplasmic reticulum or cis Golgi and stained positively with OZI (Figure 3) and peroxidase (Figure 2). Some vesicles were OZI negative and were presumably derived from trans Golgi and endosomes. Some coated vesicles appeared to contact and fuse with condensing vacuoles



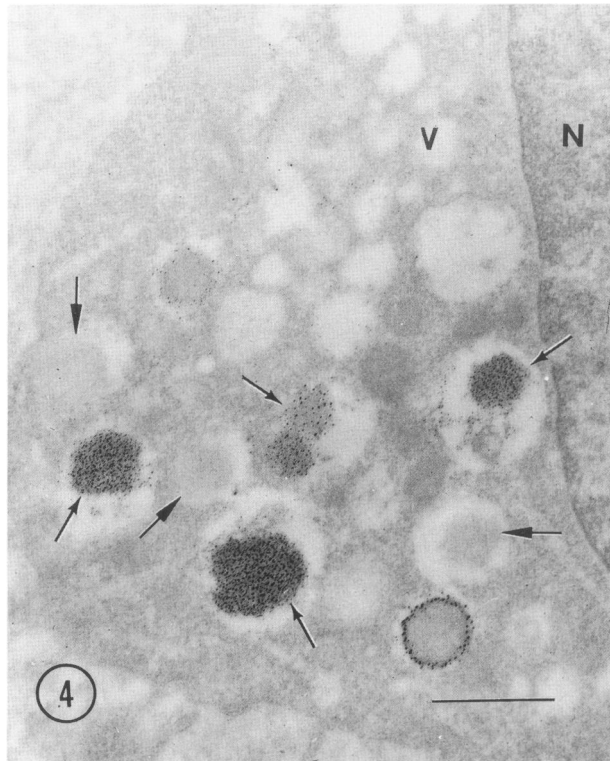


**Figure 4**—HID-TCH-SP stains sulfated glycoconjugates in central matrix material of monensin (3 hours, 1  $\mu$ M) induced expanded (preformed) granules (small arrows) in an HL60 cell. Several other incomplete granules (large arrows) and Golgi vacuoles (V) lack HID-TCH-SP staining in contrast to the positive granule staining seen in untreated HL60 cells. N, nucleus. Specimen unsmicatted. Thin section not counterstained. Bar = 1  $\mu$ .

of control HL60 cells, as well as vacuoles and incomplete granules induced by monensin treatment of HL60 cells (Figure 1).

Total protein synthesis of HL60 cells in five separate experiments was unchanged by monensin treatment (1  $\mu$ M, 16–20 hours) as measured by incorporation of  $^{35}$ S-methionine. Incorporation in treated cells was 99% (mean; range, 88–111%) of that observed in untreated cells. Furthermore, under these same conditions, there was no change in the total amount of either myeloperoxidase or  $\beta$ -glucuronidase activity associated with primary granules (means, 102 and 96%, respectively; N = 2). In marked contrast, radiolabeled sulfate incorporation and acid phosphatase activity, markers of trans-Golgi network structure and function, were observed to decrease by 82 and 65%, respectively (means; N = 2). Although myeloperoxidase and  $\beta$ -glucuronidase activities remained unchanged with monensin treatment, fractionation of subcellular organelles by Percoll density gradient centrifugation revealed significant increases in both activities associated with lower density compartments (Table 2). The data of Table 2 also show that newly synthesized, radiolabeled myeloperoxidase accumulated in lower

density compartments in monensin-treated cells. Ultrastructural analysis of these lower density Percoll fractions from both monensin-treated and untreated cells revealed an enrichment of structures resembling the incomplete granules (Figure 5b) as identified in intact monensin-treated cells (Figure 5a).

#### Early (Promyelocytes and Myelocytes) Bone Marrow Myeloid Cells

Promyelocytes could be divided into early, mid, and late stages on the basis of increasing peroxidase positive cytoplasmic granules and decreasing amounts of endoplasmic reticulum as described previously.<sup>28,29</sup> Peroxidase reactivity was observed in almost all promyelocyte granules and in endoplasmic reticulum and Golgi lamellae of many but not all promyelocytes at each stage of development.<sup>30</sup> Monensin resulted in progressive vacuolation of the promyelocyte Golgi apparatus with time and increasing monensin concentration (Figures 6, 7) similar to that seen with HL60 cells. Although many of the mature primary granules remained intact, others appeared to

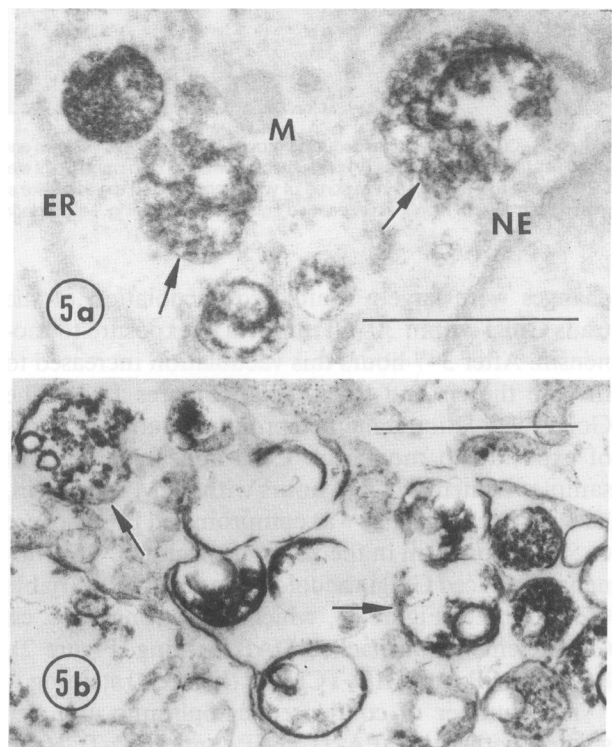


**Figure 5**—Peroxidase activity persists in the nuclear envelope (NE) and endoplasmic reticulum (ER) after 20 hours exposure of this HL60 cell to 1  $\mu$ M monensin. N, nucleus. Cytoplasmic granules contain heterogeneous material (arrows, a). An increase in these granules, presumed to be incomplete granules, was observed in lower density subcellular fractions which contained newly synthesized (radiolabeled, Table 2) myeloperoxidase (arrows, b). Thin sections not counterstained. Bar = 1  $\mu$ .

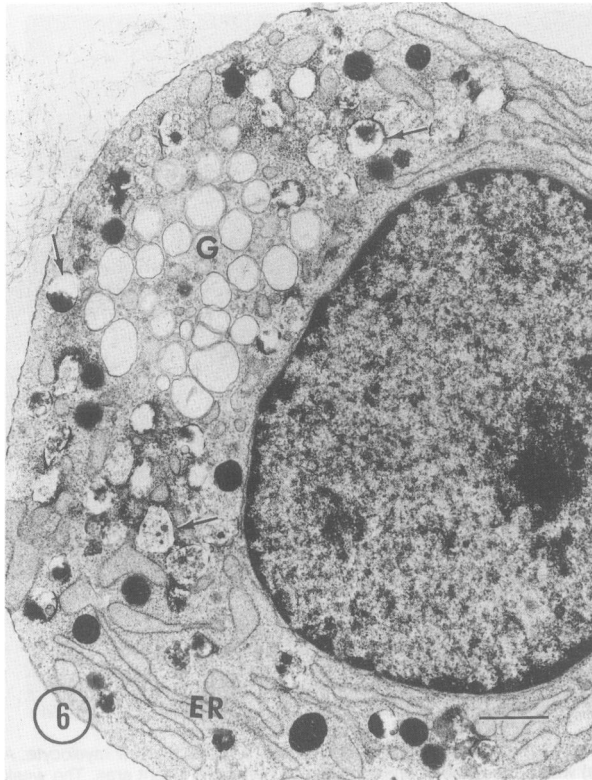


**Figure 6**—The Golgi apparatus (G) of this marrow promyelocyte appears vacuolated after exposure to 1  $\mu$ M monensin for 3 hours. Flanking cytoplasmic granules appear expanded with central and/or peripheral dense matrix material (arrows). Some granules, as well as the nuclear envelope and endoplasmic reticulum (ER), appear unaffected by the monensin. Thin section stained with uranyl acetate and lead citrate. Bar = 1  $\mu$ .

expand and demonstrated increased peripheral lucency. In some granules, a dense rim of material remained adherent to the granule membrane and was evident with UALC and peroxidase staining (Figures 6, 7) suggesting that an influx of water resulted in circumferential fracture of the matrix material. A similar pattern of granule disruption was infrequently observed in HL60 cells and was more frequent in late myeloid cells as described below. Granules containing vesicles evident in UALC and OZI stained preparations were also present but these granules were less frequent than those observed in HL60 cells. At 3–7 hours exposure to monensin, several granules appeared to fuse, resulting in large “autophagic” (or possibly heterophagic) granules with heterogeneous matrix material.

Myelocytes were identified by the presence of DAB-negative condensed granules (or secondary granules), in cells with a single (often indented) nucleus and a prominent Golgi apparatus as described previously.<sup>29,31</sup> After monensin treatment, the Golgi apparatus was vacuolated to an extent similar to that seen in promyelocytes. As in promyelocytes, subpop-

**Table 2**—Redistribution of Primary Granule Markers Following Monensin Treatment\*

	Monensin	Percent marker in subcellular fractions	
		Lower density	Higher density
<b>Myeloperoxidase</b>			
Enzyme activity	–	47	53
	+	74	26
Radiolabeled enzyme	–	48	52
	+	89	11
<b><math>\beta</math>-Glucuronidase</b>			
Enzyme activity	–	65	35
	+	79	21

\* HL60 cells were grown in culture in the presence (+) or absence (–) of 1  $\mu$ M monensin for 16–20 hours. The cells were lysed and the postnuclear supernatant was fractionated by Percoll density gradient centrifugation. Lower (0–74%) and higher (75–100%) density fractions correspond to the percent distance where 0% and 100% are the top and the bottom of the gradient, respectively. Measurements are expressed as the percentage of the total enzyme activity or immunoprecipitable radiolabeled myeloperoxidase recovered over the entire gradient. These data are from a single representative experiment. Similar distributions were observed in duplicate experiments (enzyme activity and radiolabeled enzyme) and three additional experiments in which radiolabeled enzyme alone was examined.

ulations of primary granules appeared expanded with residual matrix densities that were DAB positive and stained weakly with HID-TCH-SP and PA-TCH-SP

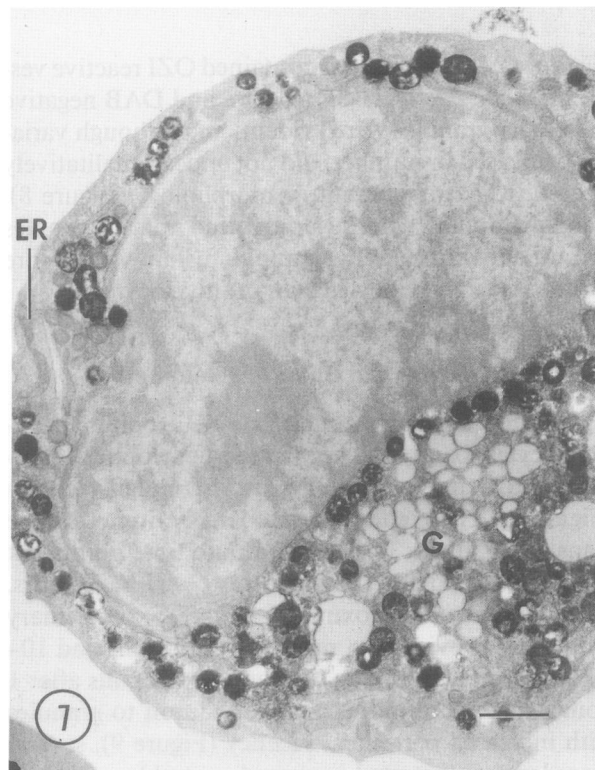


**Figure 7**—Monensin (3 hours, 1  $\mu$ M) induced Golgi vacuoles lack peroxidase staining in this marrow promyelocyte, whereas most flanking cytoplasmic granules/vacuoles stain strongly. Weak to moderate staining is evident in endoplasmic reticulum (ER). Thin section not counterstained. Bar = 1  $\mu$ .

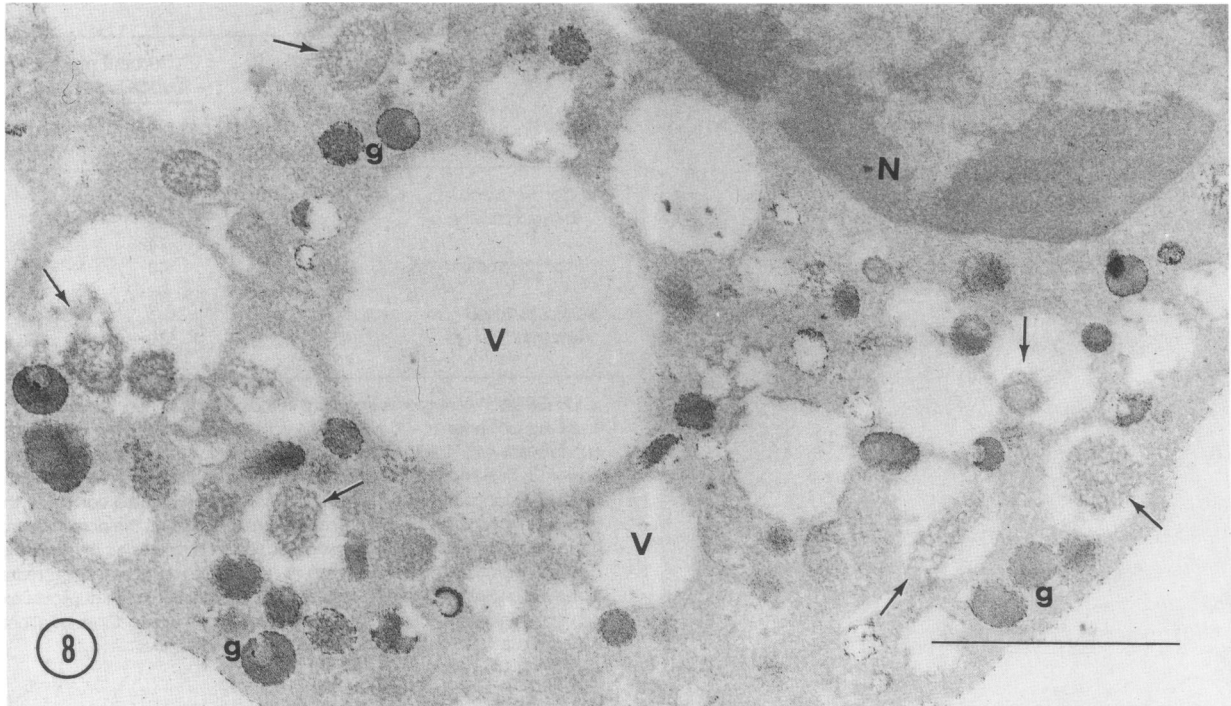


**Figure 8**—PA-TCH-SP intensely stains vicinal glycols in presumed secondary granules (g) of this monensin treated ( $1 \mu\text{M}$ , 3 hours) marrow myelocyte. A subpopulation of larger primary granules contains a weakly stained matrix (arrows) with a prominent monensin induced peripheral lucent area. The weak matrix staining is comparable to that seen in a normal subpopulation of primary granules.<sup>17</sup> Some vacuoles (V) lack matrix material. N, nucleus. Specimen not osmicated. Thin section not counterstained. Bar =  $1 \mu$ .

(Figure 8). Some granules contained OZI reactive vesiclelike foci. PA-TCH-SP reactive and DAB negative secondary granules were evident, and although variably decreased in number, did not appear qualitatively altered in matrix content or morphology (Figure 8). Larger granules with several round matrix profiles presumably formed by granule fusion were more prominent in myelocytes than promyelocytes.

#### Late Bone Marrow and Blood Myeloid Cells

After monensin treatment, late neutrophils (metamyelocytes, band, and segmented neutrophils) demonstrated a progressive increase in Golgi vacuoles (Figure 9). These changes were largely limited to the trans Golgi at the 30 and 60 minute time points but clearly involved the trans and cis Golgi at 3 hours. Vacuolation of approximately 20–30% of primary granules was evident in marrow neutrophils and 10–20% of primary granules in blood neutrophils after 1 hour exposure to monensin. In addition to granules with increased peripheral lucency (Figure 9), several granules demonstrated increased central lucency in a DAB reactive matrix (Figure 10) that had variable PA-TCH-SP and HID-TCH-SP staining. This latter granule morphology was more prominent in peripheral

blood neutrophils, whereas the former abnormal granule morphology was more prominent in marrow neutrophils. These changes were evident in 30-minute samples and increased with time. Occasional granules and/or vacuoles contained OZI reactive foci. Peroxidase-negative granules with unaltered matrix were easily identified (Figure 10), and presumably corresponded to unaltered secondary granules that were uniformly stained with UALC (Figure 9) and intensely stained with PA-TCH-SP (Figure 8). There appeared to be a small but significant decrease in these granules in some cells after 1 hour exposure to monensin. A minimal to moderate decrease in primary granules was observed and apparent fusion of primary granules occurred in many cells, resulting in the formation of large autophagic or heterophagic vacuoles containing multiple granule matrices similar to that seen in myelocytes, and less frequently in promyelocytes. These changes in late neutrophils were evident as early as 1 hour after exposure to monensin.

Control samples not exposed to monensin lacked Golgi vacuolization; however, they did contain an increase in cytoplasmic vacuoles with time including autophagic and/or heterophagic vacuoles. Nevertheless, these vacuoles were less prominent than those observed with monensin. DAB-positive granules were



generally intact and a normal subpopulation of these granules contained a central lucent angulated or crystalloid appearing area. DAB-negative granules also appeared decreased in control samples without monensin, particularly 3 or more hours after incubation. A loss of granules was more prominent in monensin treated cells but the decrease in granules in controls prevented clear interpretation of this result.

### Discussion

This study demonstrates that monensin alters neutrophil morphology and granule genesis. The disruption of the  $\text{Na}^+/\text{H}^+$  antiporter in the trans Golgi, condensing vacuoles, and maturing primary granules results in emergence of an abnormal pattern of primary granule genesis in human myeloid cells. Thus, while packaging of granule components in normal myeloid cells involves movement of proteins through endoplasmic reticulum, Golgi lamellae, and condensing vacuoles (Figure 11), monensin treatment appears to block movement in the latter compartments. This resulted in altered trafficking of endoplasmic reticulum-derived components with the appearance of a mor-

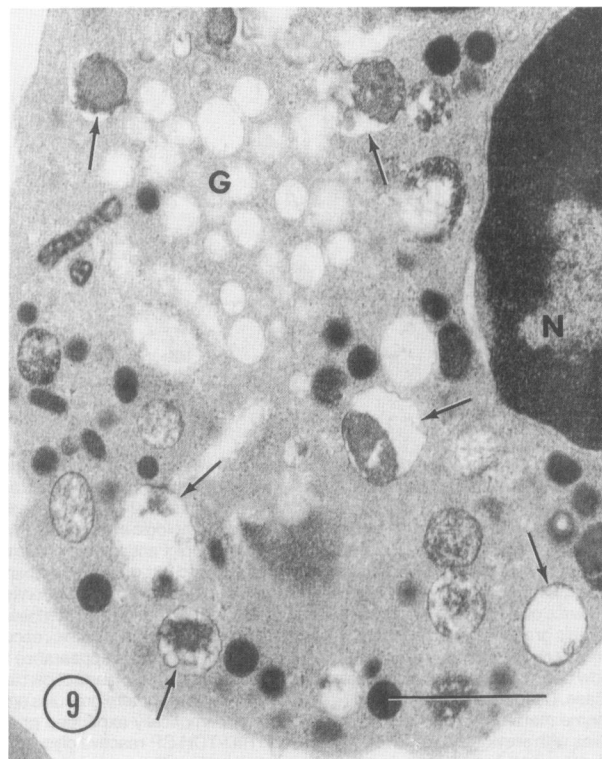


**Figure 9**—This segmented neutrophil from a marrow specimen contains a prominent vacuolated Golgi (G) region as a result of monensin treatment ( $1 \mu\text{M}$ , 3 hours). Several primary granules appear expanded with variably distributed matrix material (arrows). Smaller granules, some of which are secondary granules, lack morphologic abnormalities. N, nucleus. Thin section stained with uranyl acetate and lead citrate. Bar =  $1 \mu$ .

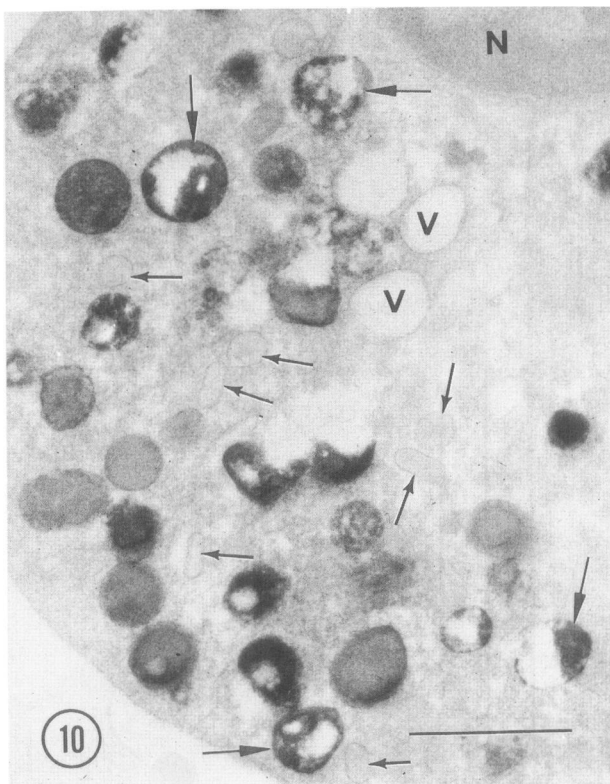


**Figure 10**—This peripheral blood segmented neutrophil stained for peroxidase contains monensin ( $1 \mu\text{M}$ , 3 hours) induced expanded peroxidase positive granules with increased matrix lucencies (large arrows). Secondary granules lack staining (small arrows) and their matrix material appears unaltered by monensin. A few enlarged cytoplasmic vacuoles (V) are presumably Golgi derived. N, nucleus. Thin section not counterstained. Bar =  $1 \mu$ .

phologically and cytochemically unique incomplete granule that fractionated with newly synthesized peroxidase and lacked Golgi-contributed  $^{35}\text{SO}_4$  and HID-reactive glycoconjugates. The monensin-induced dissociation of acidic compartments from other steps in granule genesis provides a model for primary granule genesis emphasizing granule heterogeneity and the potential for complex addition of granule components from a variety of cell organelles (Figure 12).

Vacuolation of Golgi lamellae is the predominant morphologic insult described in previous biochemical and ultrastructural studies of HL60 cells,<sup>26</sup> blood neutrophils,<sup>9</sup> and secretory cells.<sup>6</sup> The early effect of monensin on the trans Golgi is consistent with the acidic nature of this subcellular compartment observed in other cell types.<sup>6</sup> The osmotic insult to the Golgi lamellae results in the accumulation of vacuoles, which lack HID-TCH-SP and PA-TCH-SP staining, consistent with monensin-induced inhibition of processing of sulfated and vicinal glycol containing glycoconjugates in the trans Golgi. The significant decrease in  $^{35}\text{SO}_4$  incorporation into monensin-treated HL60 cells is consistent with the cytochemical observation

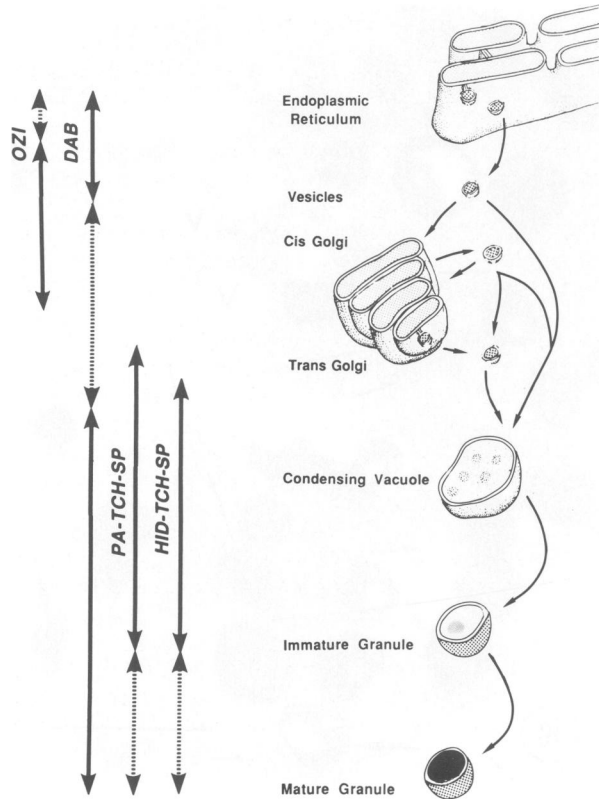


**Figure 11**—This schematic diagram presents a model for multiple pathways of addition of granule components during formation of peroxidase positive granules in promyelocytes not exposed to monensin. OZI stains reducing substances (eg, sulfhydryl groups) in endoplasmic reticulum (in normal promyelocytes but not HL60 cells, as depicted by dotted lines), some cytoplasmic vesicles, and components of the cis Golgi, but fails to stain trans Golgi components. DAB stains myeloperoxidase in all subcellular compartments depicted in normal promyelocytes but fails to similarly stain Golgi lamellae in control HL60 cells, as depicted by dotted lines and reported previously.<sup>23,37</sup> Transport of material from cis Golgi directly to condensing vacuoles is suggested based upon the present OZI staining results in monensin treated cells and DAB staining in HL60 cells, however, the lack of OZI staining in normal condensing vacuoles/immature granules would suggest that the added material is rapidly processed. Glycoconjugate staining with PA-TCH-SP and HID-TCH-SP is apparent in the pathway involving trans Golgi and immature granules<sup>17,20,32</sup>; however, this staining is masked or lost (in normal promyelocytes but not untreated HL60 cells) with granule maturation (dotted lines). This hypothesis proposes that developing primary granules receive macromolecules directly from a variety of Golgi compartments and possibly endoplasmic reticulum.

of decreased HID-TCH-SP staining of promyelocyte granules in this study and indicates that the decreased staining is due to decreased glycoconjugate production rather than extraction or masking of histochemically reactive components.

Transport of endoplasmic reticulum-derived substances to the incomplete granules presumably occurs through cytoplasmic vesicles, some or all of which may be coated vesicles.<sup>28</sup> This is supported by the fact that these vesicles demonstrate OZI staining found in endoplasmic reticulum and cis Golgi elements but not trans Golgi elements.<sup>6,18</sup> Accumulation of OZI reactive material in granules/vacuoles of monensin

treated cells is consistent with the morphologic observation of similar structures in monensin-treated pancreatic cells.<sup>6,7</sup> Thus, these results would suggest that the neutrophil primary granule receives macromolecular components directly through endoplasmic reticulum/cis Golgi-derived vesicles, as well as through trans Golgi-derived, vicinal-glycol-containing, tubulovesicular structures, and separate sulfate-containing spherules or vesicles as previously described.<sup>17,20,32</sup>

The present and previous studies<sup>26,33</sup> demonstrate normal levels of production of endoplasmic reticu-

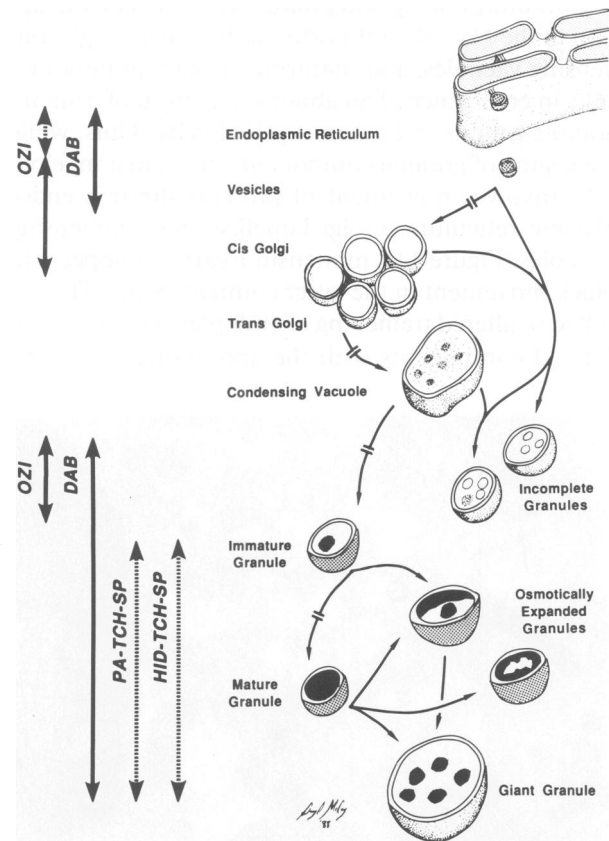


**Figure 12**—This diagram depicts the stages at which monensin exerts an effect on the formation of peroxidase-positive granules in promyelocytes. Interrupted lines indicate disruption of normal pathways of granule genesis resulting in alternate pathways and formation of pathologic structures (uninterrupted lines). Monensin disrupts trans and cis Golgi antiporters preventing or limiting movement of macromolecules into and out of these compartments. An incomplete granule lacking glycoconjugates is formed as a consequence of lack of addition of trans Golgi components. The *de novo* synthesis of this granule is suggested by its content of presumed endoplasmic reticulum derived peroxidase-reactive OZI-reactive material and its appearance in low density cell fractions containing newly synthesized (radiolabeled) peroxidase. Disruption of a presumed Na<sup>+</sup>/H<sup>+</sup> antiporter in immature granules and some mature granules results in formation of osmotically expanded granules with previously added PA-TCH-SP and HID-TCH-SP-reactive glycoconjugates and further granule maturation is prevented. The expanding granule(s) with or without membrane damage may then fuse with other granules, resulting in giant granule formation (ie, autophagy/heterophagy) with multiple cores of matrix material. Thus, this hypothesis suggests that a monensin sensitive Na<sup>+</sup>/H<sup>+</sup> antiporter is present in Golgi lamellae, condensing vacuoles, immature primary granules, and a subpopulation of mature primary granules, whereas endoplasmic reticulum and some mature cytoplasmic granules lack this antiporter.

lum-derived myeloperoxidase and  $\beta$ -glucuronidase in monensin-treated cells despite the marked reduction of trans Golgi contributed acid phosphatase and sulfated glycoconjugates ( $^{35}\text{SO}_4$  incorporation and HIDA-TCH-SP-staining) after monensin treatment. Localization of newly synthesized (precursor) myeloperoxidase in lower density compartments containing increased numbers of incomplete granules, together with the unique morphology and cytochemistry of these organelles, suggests incomplete granules are synthesized *de novo*. Consistent with this idea are the observations that forming primary granules in normal promyelocytes appear to bud off the cis face of the Golgi<sup>29</sup> and swainsonine, an inhibitor of mannosidase II<sup>34</sup> localized to medial Golgi cisternae,<sup>35</sup> has no effect on the processing of myeloperoxidase precursors in HL60 cells.<sup>36</sup> The observed relative lack of peroxidase staining in HL60 Golgi lamellae is consistent with a pathway that does not include the trans Golgi.<sup>27,37</sup> Nevertheless, the observation of positive DAB staining of all Golgi lamellae in normal promyelocytes<sup>38</sup> indicates that the processing of peroxidase is complex and may involve more than one subcellular pathway. Other peroxidase preparations using a different staining technique have demonstrated a DAB-negative granule precursor to which peroxidase activity is imparted later in granule genesis,<sup>39</sup> suggesting sequential addition of granule components in at least some promyelocyte granules. Further studies are needed to determine if different pathways may be correlated with the multiple forms of myeloperoxidase, described previously in neutrophilic granulocytes,<sup>24</sup> and if these are related in turn to the multiple forms of peroxidase positive granules also seen in these cells.<sup>40-42</sup>

The observed expansion of some preformed primary granules and their corresponding increased peripheral lucency is consistent with  $\text{H}_2\text{O}$  influx in an osmotic insult after monensin disruption of the  $\text{Na}^+/\text{H}^+$  antiporter. This relatively selective effect appears to identify a subpopulation of primary granules and distinguishes these granules from other primary granules as well as secondary granules. The formation of giant granules with heterogeneous content in cells exposed to monensin for prolonged periods indicates granule fusion has occurred. The progressive decrease (with time) in cytoplasmic granules observed with monensin exposure may be the result of degranulation into the extracellular space, autophagic vacuoles, or both. Previous studies have demonstrated minimal but significant decreases in primary and secondary granule markers of monensin treated neutrophils<sup>9</sup> consistent with the relative decrease in granules observed in the present study.

## References

1. Mellman I, Fuchs R, Helenius A: Acidification of the endocytic and exocytic pathways. *Ann Rev Biochem* 1986, 55:663-700
2. Forgac M, Cantley L: Characterization of the ATP-dependent proton pump of clathrin-coated vesicles. *J Biol Chem* 1984, 259:8101-8105
3. Zhang F, Schneider DL: The bioenergetics of Golgi apparatus function: Evidence for an ATP-dependent proton pump. *Biochem Biophys Res Commun* 1983, 114: 620-625
4. Schneider DL: ATP-dependent acidification of intact and disrupted lysosomes: Evidence for an ATP-driven proton pump. *J Biol Chem* 1981, 256:3858-3864
5. Scherman D, Nordmann J, Henry JP: Existence of an adenosine 5'-triphosphate dependent proton translocase in bovine neurosecretory granule membrane. *Biochem* 1982, 21:687-694
6. Orci L, Halban P, Amherdt M, Ravazzola M, Vassalli JD, Perrelet A: A clathrin-coated, Golgi-related compartment of the insulin secreting cell accumulates proinsulin in the presence of monensin. *Cell* 1984, 39:39-47
7. Orci L, Ravazzola M, Amherdt M, Madsen O, Perrelet A, Vassalli JD, Anderson RGW: Conversion of proinsulin to insulin occurs coordinately with acidification of maturing secretory vesicles. *J Cell Biol* 1986, 103: 2273-2281
8. Lemansky P, Hasilik A, von Figura K, Helmy S, Fishman J, Fine RE, Kedersha NL, Rome LH: Lysosomal enzyme precursors in coated vesicles derived from the exocytic and endocytic pathways. *J Cell Biol* 1987, 104: 1743-1748
9. Jesaitis RK, Dahinden CA, Chang CM, Jesaitis AJ: Investigations on the role of Golgi-mediated, ligand-receptor processing in the activation of granulocytes by chemoattractants: Differential effects of monensin. *Biochim Biophys Acta* 1987, 927:382-391
10. Montalvo EA, Parmley RT, Grose C: Structural analysis of the varicella-zoster virus gp98-gp62 complex: Posttranslational addition of N-linked and O-linked oligosaccharide moieties. *J Virol* 1985, 53:761-770
11. Akin DT, Kinkade JM Jr: Evidence for the involvement of an acidic compartment in the processing of myeloperoxidase in human promyelocytic leukemia HL60 cells. *Arch Biochem Biophys* 1987, 255:428-436
12. Wright J, Schwartz JH, Olson R, Kosowsky JM, Tauber AL: Proton secretion by the sodium/hydrogen ion antiporter in the human neutrophil. *J Clin Invest* 1986, 77: 782-788
13. Simchowitz L: Chemotactic Factor-induced activation of  $\text{Na}^+/\text{H}^+$  exchange in human neutrophils: I. Sodium fluxes. *J Biol Chem* 1985, 260:13237-13247
14. Simchowitz L: Chemotactic factor-induced activation of  $\text{Na}^+/\text{H}^+$  exchange in human neutrophils: II. Intracellular pH changes. *J Biol Chem* 1986, 260:13248-13255
15. Parmley RT, Akin DT, Kinkade JM Jr: Monensin disrupts neutrophil granule genesis and a selective subset of primary granules. *Blood* 1987, 70(Suppl. 1):94
16. Graham RC Jr, Karnovsky MJ: The early stages of absorption of injected horseradish peroxidase in the proximal tubules of mouse kidney: Ultrastructural cyto-

- chemistry by a new technique. *J Histochem Cytochem* 1966, 14:291-302
17. Fittschen C, Parmley RT, Austin RL, Crist WM: Vicinal glycol-staining identifies secondary granules in human normal and Chédiak-Higashi neutrophils. *Anat Rec* 1983, 205:301-311
  18. Clark MA, Ackerman GA: Osmium-zinc iodide reactivity in human blood and bone marrow cells. *Anat Rec* 1971, 170:81-96
  19. Spicer SS: Diamine methods for differentiating mucosubstances histochemically. *J Histochem Cytochem* 1965, 13:211-234
  20. Parmley RT, Hurst RE, Takagi M, Spicer SS, Austin RL: Glycosaminoglycans in human neutrophils and leukemic myeloblasts: Ultrastructural, cytochemical, immunologic, and biochemical characterization. *Blood* 1983, 61:257-266
  21. Thiéry JP: Mise en évidence des polysaccharides sur coupes fines en microscopie électronique. *J Microsc* 1967, 6:987-1018
  22. Sannes PL, Spicer SS, Katsuyama T: Ultrastructural localization of sulfated complex carbohydrates with a modified iron diamine procedure. *J Histochem Cytochem* 1979, 27:1108-1111
  23. Akin DT, Kinkade JM Jr: Processing of a newly identified intermediate of human myeloperoxidase in isolated granules occurs at neutral pH. *J Biol Chem* 1986, 261:8370-8375
  24. Pember SO, Shapira R, Kinkade JM Jr: Multiple forms of myeloperoxidase from human neutrophilic granulocytes: Evidence for differences in compartmentalization, enzymatic activity, and subunit structure. *Arch Biochem Biophys* 1983, 221:391-403
  25. Pember SO, Kinkade JM Jr: Differences in myeloperoxidase activity from neutrophilic polymorphonuclear leukocytes of differing density: Relationship to selective exocytosis of distinct forms of the enzyme. *Blood* 1983, 61:1116-1124
  26. Akin DT, Kinkade JM Jr, Parmley RT: Biochemical and ultrastructural effects of monensin on the processing, intracellular transport, and packaging of myeloperoxidase into low and high density compartments of human leukemia (HL60) cells. *Arch Biochem Biophys* 1987, 257:451-463
  27. Parmley RT, Akin DT, Barton JC, Gilbert CS, Kinkade JM Jr: Cytochemistry and ultrastructural morphology of cultured HL60 myeloid leukemia cells. *Cancer Res* 1987, 47:4932-4940
  28. Ackerman GA: The human neutrophilic promyelocyte: A correlated phase and electron microscopic study. *Z Zellforsch* 1971, 118:467-481
  29. Bainton DF, Ulliyot JL, Farquahr MG: The development of neutrophilic polymorphonuclear leukocytes in human bone marrow. *J Exp Med* 1971, 134:907-934
  30. Dunn WB, Hardin JH, Spicer SS: Ultrastructural localization of myeloperoxidase in human neutrophil and rabbit heterophil and eosinophil leukocytes. *Blood* 1968, 32:935-944
  31. Ackerman GA: The human neutrophilic myelocyte: A correlated phase and electron microscopic study. *Z Zellforsch* 1971, 121:153-170
  32. Parmley RT, Eguchi M, Spicer SS, Alvarez C, Austin RL: Ultrastructural cytochemistry and radioautography of complex carbohydrates in heterophil granulocytes from rabbit bone marrow. *J Histochem Cytochem* 1980, 28:1067-1080
  33. Olsson I, Lantz M, Persson AM, Arnljots K: Biosynthesis and processing of lactoferrin in bone marrow cells, a comparison with processing of myeloperoxidase. *Blood* 1988, 71:441-447
  34. Elbein AD: Inhibitors of the biosynthesis and processing of N-linked oligosaccharide chains. *Ann Rev Biochem* 1987, 56:497-534
  35. Kornfeld R, Kornfeld S: Assembly of asparagine-linked oligosaccharides. *Ann Rev Biochem* 1985, 54:631-664
  36. Nauseef WM: Posttranslational processing of a human myeloid lysosomal protein, myeloperoxidase. *Blood* 1987, 70:1143-1150
  37. Bainton DF: HL60 cells have abnormal myeloperoxidase transport and packaging. *Exp Hemat* 1988, 16:150-158
  38. Ackerman GA, Clark MA: Ultrastructural localization of peroxidase activity in normal human bone marrow cells. *Z Zellforsch* 1971, 117:463-475
  39. Brederoo P, Van der Meulen J, Daems W: Ultrastructural localization of peroxidase activity in developing neutrophil granulocytes from human bone marrow. *Histochem* 1986, 84:445-453
  40. Rice WG, Kinkade JM Jr, Parmley RT: High resolution of heterogeneity among human neutrophil granules: Physical, biochemical, and ultrastructural properties of isolated fractions. *Blood* 1986, 68:541-555
  41. Rice WG, Ganz T, Kinkade JM Jr, Selsted ME, Lehrer RI, Parmley RT: Defensin-rich dense granules of human neutrophils. *Blood* 1987, 70:757-765
  42. Parmley RT, Rice WG, Kinkade JM Jr, Gilbert C, Barton JC: Peroxidase-containing microgranules in human neutrophils: Physical, morphological, cytochemical, and secretory properties. *Blood* 1987, 70:1630-1638

### Acknowledgment

The authors thank Drs. W. R. Vogler, E. F. Winton, and the staff of the Cell Separator Department (Emory University Hospital) for assisting in the processing of blood and bone marrow specimens. They also thank Daryl McCoy for his artwork and Ms. Ester Alvear and Ms. Maxine Swan for their expert secretarial assistance.